

Chapter 6

Peer-to-Peer Energy Transactions in Active Distribution Systems: A Kalai-Smorodinsky Bargaining Framework

6.1 Introduction

The previous chapter deals with the Nash bargaining-based framework, and DSO maintains the network constraints with the help of DGs, which are under the control of DSO. This work proposes a novel P2P energy-sharing framework using a modified Nash bargaining-based cooperative game for all buildings hypothetically aggregated as virtual communities (VCs) based on their location in the distribution network. This framework incorporates the active participation of DGs as well as DSO in the local energy market and has the ability to settle transactions maintaining the network constraints through dynamic network usage charges and electricity prices. The hypothetical aggregation or grouping (virtual community) reduces the number of transactions, resulting in improved computational efficiency and scalability. The building model used in this chapter is more realistic than that used in previous chapters. The proposed algorithm is based on cloud computing which can derive the equilibrium strategies of all players using a privacy-preserving decentralised approach. The formulation proposed in the present chapter addresses the above points in the following way.

- The proposed formulation introduces dynamic network usage charges so that the transactions can be fine-tuned vis-a-vis technical constraints.
- A cloud-based arrangement is made which communicates the net injection at a bus to the DSO, thereby avoiding the sharing of any sensitive information between the DSO and the participants and consequently avoiding security and privacy issues.
- The effect of active participation of DGs on the LMP in the proposed framework has also been investigated in two scenarios, viz., the dispatchable DGs bid into the energy market, and the DGs supply to the system on a marginal cost basis.
- A modified form of Nash Bargaining is used in this P2P energy-trading framework.

6.2 Problem Formulation

6.2.1 System Model

Figure 6.1 shows the schematic diagram of the local energy trading. This framework assumes robust communication infrastructure and a secure separate platform for limited information sharing and cloud computing. Each building is assumed to be equipped with demand-responsive load, RES, and smart meters. The virtual community (VC) on a bus consists of all buildings, B_i , and BESS on that bus. Here, the VC is a hypothetical aggregation of buildings and BESS connected through a computing cloud. Each VC is connected through a computing cloud for C2C exchange. The virtual communities are considered profit-based entities for C2C trading and are considered non-profit-based entities for their own buildings. This concept utilises the advantage of P2P trading between buildings with less communication and computational burden without affecting the total profit of buildings. Also, managing a shareable BESS using a VC cloud is more convenient. The computing cloud in each VC is used to deal with coupled decisions of different entities required for following.

- i) Trading with utility and other VCs (C2C),
- ii) Charging/discharging of BESS,
- iii) Exchanging power between the buildings (B2B), and
- iv) Exchanging power between the buildings and VC (B2C).

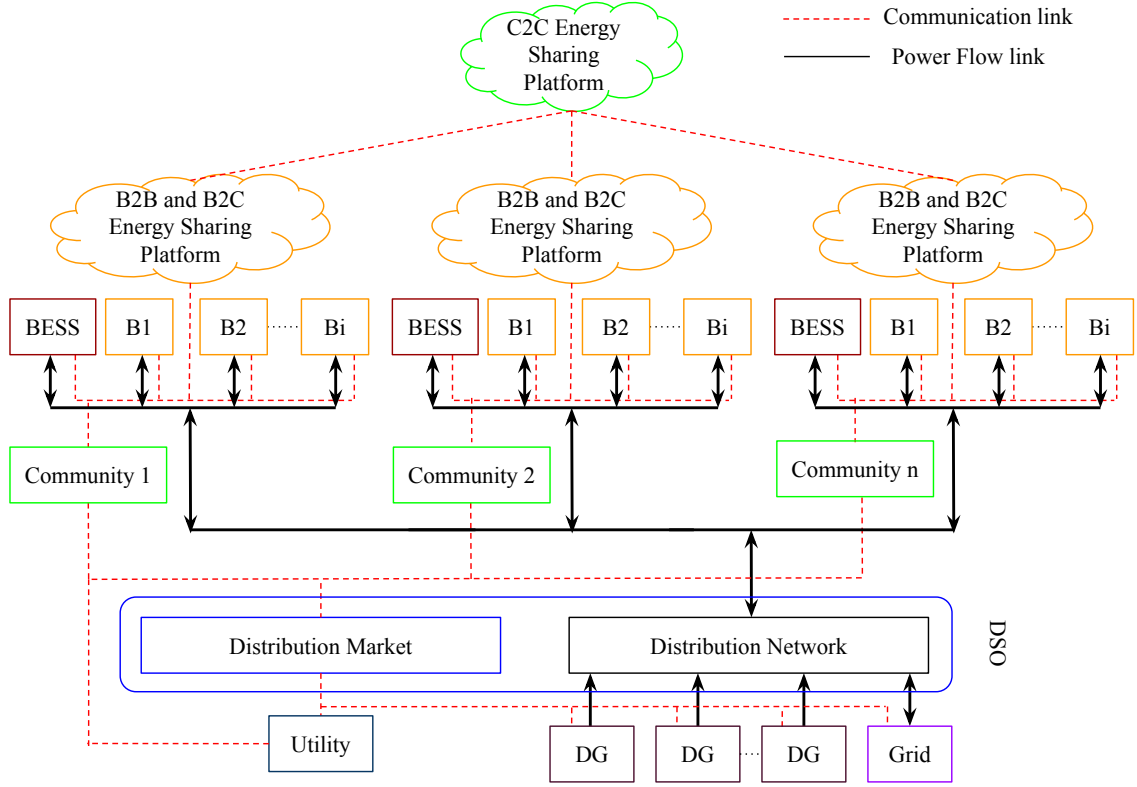


Figure 6.1: CLOUD COMPUTING BASED PEER-TO-PEER ENERGY SHARING FRAMEWORK

Also, this framework considers an active distribution system in which DGs and buildings are on different buses. The proposed framework considers the active participation of prosumers and producers. DGs offer their bidding strategy based on the LMPs received from DSO. The DSO is responsible for clearing the local distribution market by assessing each VC's net power injection and the bidding strategies of DGs. The DSO is also accountable for maintaining the network parameters within limits. This framework can be sub-modelled into buildings, VCs, DGs, and DSO.

6.2.2 Building

The aim of a building is to minimise the cost of discomfort (arising due to shifting of load and deviation from the reference temperature) and meet its demand with the help of B2B and B2C energy trading. The total cost of i^{th} building of n^{th} VC can be represented as

$$C_{n,i}^b = \sum_{t=1}^T (C_{n,i,t}^{ls} + C_{n,i,t}^{HVAC}) + C_{n,i}^{b2b} + C_{n,i}^{b2c}, \quad (6.1)$$

where,

$$C_{n,i,t}^{ls} = \Lambda_t^{disc} (P_{n,i,t}^{ls} - L_{n,i,t}^A)^2, \quad (6.2)$$

$$C_{n,i,t}^{HVAC} = \Lambda_t^{HVAC} (T_{p_{n,i,t}}^{HVAC} - T_{p_{n,i,t}}^r)^2, \quad (6.3)$$

$$C_{n,i}^{b2b} = \sum_{\substack{j=1 \\ j \neq i}}^{N_n^b} \pi_{n,i,j}^{b2b}, \quad \text{and} \quad (6.4)$$

$$C_{n,i}^{b2c} = \pi_{n,i}^{b2c}. \quad (6.5)$$

Here, $C_{n,i,t}^{ls}$, $C_{n,i,t}^{HVAC}$, $C_{n,i}^{b2b}$, and $C_{n,i}^{b2c}$ are the cost of discomfort due to load shifting, cost of discomfort due to deviation from the reference temperature, energy cost related to B2B trading, and B2C trading respectively. The constraints associated with the building-level problem are as follows.

$$L_{n,i,t}^{min} \leq P_{n,i,t}^{ls} \leq L_{n,i,t}^{max}, \quad (6.6)$$

$$\sum_{t=1}^T P_{n,i,t}^{ls} \geq \epsilon^{LS} \sum_{t=1}^T L_{n,i,t}^A, \quad (6.7)$$

$$T_{p_{n,i,t}}^{min} \leq T_{p_{n,i,t}}^{HVAC} \leq T_{p_{n,i,t}}^{max}, \quad (6.8)$$

$$T_{p_{n,i,t+1}}^{HVAC} = (h^a T_{p_{n,i,t}}^{HVAC}) + (h^b T_{p_{n,i,t}}^O) + (h^c P_{n,i,t}^{HVAC}), \quad (6.9)$$

$$P_{n,i,j,t}^{b2b} + P_{n,j,i,t}^{b2b} = 0, \quad (6.10)$$

$$\pi_{n,i,j}^{b2b} + \pi_{n,j,i}^{b2b} = 0, \quad (6.11)$$

$$-\sum_{\substack{j=1 \\ j \neq i}}^{N_n^b} P_{n,i,j,t}^{b2b} - P_{n,i,t}^{b2c} = R_{n,i,t} - P_{n,i,t}^{ls} - P_{n,i,t}^{HVAC}, \quad \text{and} \quad (6.12)$$

$$C_{n,i}^{b0} - C_{n,i}^b \geq 0. \quad (6.13)$$

The load shifting limits and the maximum allowable curtailment of the load are given by (6.6) and (6.7), respectively. The value of ϵ^{LS} equals 1 in case there is no load curtailed. To maintain the indoor temperature ($T_{p_{n,i,t}}^{HVAC}$) within the acceptable range, equation (6.8) is used. Equation (6.9) describes the dynamics of indoor temperature in heating mode [82]. The temperature of the outside environment and the electric power input is given by $T_{p_{n,i,t}}^O$ and $P_{n,i,t}^{HVAC}$ respectively. For B2B trading, the power and incentive equilibrium constraints (6.10) and (6.11) are the coupling constraints between i^{th} and j^{th} buildings. If the i^{th} building receives incentive from j^{th} building, then the incentive $\pi_{n,i,j}^{b2b}$ will be negative otherwise positive. The power exchange in B2B sharing, $P_{n,i,j,t}^{b2b}$, and B2C sharing, $P_{n,i,t}^{b2c}$, are considered as positive if i^{th} building imports power from

j^{th} building or from its VC. Similarly, the negative values of $P_{n,i,j,t}^{b2b}$ and $P_{n,i,t}^{b2c}$ indicate power exports. Considering RESs power, load shifting, and power exchange with the VC and other buildings, the power balancing equation can be defined as (6.12). The building will participate in internal trade only if it has the opportunity to reduce operating costs. Therefore, constraint (6.13) is used to ensure the benefit of the building. The term $C_{n,i}^{b0}$ represents the cost of building without internal trading (exchange power with utility only).

6.2.3 Virtual Community (VC)

Similar to the buildings, the hypothetical entities, i.e., virtual communities, aim to minimise their cost function, C_n^c , which includes cost due to trade with utility, $C_{n,t}^U$, battery utilisation cost, $C_{n,t}^{BESS}$, and due to community-to-community (C2C) trade with other VCs, C_n^{c2c} . For n^{th} VC at time t , the cost function, C_n^c is given by,

$$C_n^c = \sum_{t=1}^T (C_{n,t}^U + C_{n,t}^{BESS}) + C_n^{c2c}, \quad (6.14)$$

where

$$C_{n,t}^U = (\Lambda_{n,t}^{im} + \epsilon^{CE})P_{n,t}^b - \Lambda_{n,t}^{ex}P_{n,t}^s, \quad (6.15)$$

$$C_{n,t}^{BESS} = \Lambda^{UTI}(P_{n,t}^{ch} + P_{n,t}^{dis}), \quad \text{and} \quad (6.16)$$

$$C_n^{c2c} = \sum_{\substack{m=1 \\ m \neq n}}^{N^c} \left(\sum_{t=1}^T \Lambda_{n,m,t}^{NUC} P_{n,m,t}^{c2c} + \pi_{n,m} \right). \quad (6.17)$$

The constraints associated with the VC-level are as follows.

$$P_n^{ch_{min}} \leq P_{n,t}^{ch} \leq P_n^{ch_{max}}, \quad (6.18)$$

$$P_n^{dis_{min}} \leq P_{n,t}^{dis} \leq P_n^{dis_{max}}, \quad (6.19)$$

$$SOC_{n,t} = (1 - \eta_n^{loss})SOC_{n,t-1} + \eta_n^{ch}P_{n,t}^{ch} - \frac{1}{\eta_n^{dis}}P_{n,t}^{dis}, \quad (6.20)$$

$$SOC_n^{min} \leq SOC_{n,t} \leq SOC_n^{max}, \quad (6.21)$$

$$C_n^{c0} - C_n^c \geq 0, \quad (6.22)$$

$$P_{n,m,t}^{c2c} + P_{m,n,t}^{c2c} = 0, \quad (6.23)$$

$$\pi_{n,m}^{c2c} + \pi_{m,n}^{c2c} = 0, \quad (6.24)$$

$$P_{n,t}^b - P_{n,t}^s + P_{n,t}^{dis} - P_{n,t}^{ch} + \sum_{\substack{m=1 \\ m \neq n}}^{N^c} P_{n,m,t}^{c2c} = \sum_{i=1}^{N_n^b} P_{n,i,t}^{b2c}, \quad \text{and} \quad (6.25)$$

$$C_n^c = \sum_{i=1}^{N_n^b} \pi_{n,i}^{b2c}. \quad (6.26)$$

For n^{th} VC, the cost of power exchange with the utility is given by (6.15). Here, $P_{n,t}^b$ and $P_{n,t}^s$ are the power bought (imported) and sold (exported) from the utility. The prices of power import, $\Lambda_{n,t}^{im}$, and export, $\Lambda_{n,t}^{ex}$, are based on the LMP of the k^{th} bus on which the VC is present. If the VC is present on bus then $\Lambda_{n,t}^{im} = a\lambda_{t,k}^{LMP}$ and $\Lambda_{n,t}^{ex} = \Lambda_{n,t}^{im}/\epsilon^R$. The scaling factors a and ϵ^R are utility-driven parameters. The battery utilisation cost is given by (6.16). This cost accounts for the degradation of BESS caused by its repetitive charging and discharging.

Internal trading incorporated in this work enhances the effectiveness of RESs and BESSs. At this level, C2C trading provides such results. The $P_{n,m,t}^{c2c}$ and $\pi_{n,m}^{c2c}$ is positive when n^{th} VC is importing from m^{th} VC. In the case of power export from the n^{th} VC, $P_{n,m,t}^{c2c}$ will be negative. The total cost for inter-community (C2C) energy trading is given by (6.17). The first term of (6.17) is the network utilisation charge (NUC). The $\Lambda_{n,m,t}^{NUC}$ is given by the following equation.

$$\Lambda_{n,m,t}^{NUC} = \begin{cases} \frac{1}{2} \max(\lambda_{t,n}^{LMP} - \lambda_{t,m}^{LMP}) & \text{if } P_{n,m,t}^{c2c} \geq 0 \text{ and } (\lambda_{t,n}^{LMP} - \lambda_{t,m}^{LMP}) \geq 0, \\ 0 & \text{if } P_{n,m,t}^{c2c} \geq 0 \text{ and } (\lambda_{t,n}^{LMP} - \lambda_{t,m}^{LMP}) < 0, \\ \frac{1}{2} \max(\lambda_{t,m}^{LMP} - \lambda_{t,n}^{LMP}) & \text{if } P_{n,m,t}^{c2c} < 0 \text{ and } (\lambda_{t,m}^{LMP} - \lambda_{t,n}^{LMP}) \geq 0, \\ 0 & \text{if } P_{n,m,t}^{c2c} < 0 \text{ and } (\lambda_{t,m}^{LMP} - \lambda_{t,n}^{LMP}) < 0. \end{cases}$$

According to the above equation, the Network Utilization Charge (NUC) is applied when power is exported from a higher LMP bus to a lower LMP bus. The LMPs are determined using Optimal Power Flow (OPF), which considers voltage levels, line limits, and other relevant factors. If a peer-to-peer (P2P) energy exchange violates any system constraints, this is reflected in the LMP, leading to an increase in the NUC. The higher NUC then discourages excessive power exchange, prompting communities to adjust their exchanged power values. These updated values are subsequently used in the next OPF calculation. This iterative process continues until the difference between successive LMP values falls within an acceptable tolerance. In this way, the NUC helps manage line loading and voltage limits effectively.

The second term of (6.17) is the incentives received/paid for C2C energy trading. The charging/discharging power of the BESS is limited by (6.18) and (6.19). The state-of-charge, $SOC_{n,t}$, for a BESS of n^{th} VC at a time t depends on the SOC at time $(t - 1)$ and charging/discharging power level as given in (6.20). The SOC level is constrained by (6.21). The

constraint (6.22) ensures the benefit of the VC in C2C trading. Here, C_n^{c0} is the cost value of the VC without C2C energy trading. The constraints (6.23) and (6.24) represent the power and incentive balancing for C2C trading between n^{th} and m^{th} VCs. The load balancing constraint at the VC level is given in (6.25). Equation (6.26) shows that the B2C incentive distribution among the buildings equals the total cost of a non-profit-based VC. This framework doesn't need any separate constraints to prevent simultaneous charging and discharging or buying and selling to the grid, as explained in Appendix III.

6.2.4 DGs

In this proposed work, the DGs are considered separate entities that offer their bids to the DSO. The DGs participate in the usual energy market (main market) as well as coordinate with DSO through the ancillary market for supplementary operations. To maximise the profit, the objective function of DGs can be defined as the minimization of the difference of the cost of generation and revenue earned from selling. The objective function, C_d^{DG} , of d^{th} DG can be written as,

$$C_d^{DG} = \sum_{t=1}^T [c_d^a + c_d^b(P_{d,t}^M + P_{d,t}^S) + c_d^c(P_{d,t}^M + P_{d,t}^S)^2 - \Lambda_{d,t}^M P_{d,t}^M - \Lambda_{d,t}^S P_{d,t}^S], \quad (6.27)$$

where,

$$P_d^{min} \leq P_{d,t}^M + P_{d,t}^S \leq P_d^{max}. \quad (6.28)$$

Here, c_d^a , c_d^b , and c_d^c are the cost-characteristic parameters of DG. $P_{d,t}^M$ and $P_{d,t}^S$ are the power sold by DG to DSO in the main market and during supplementary operations, respectively. P_d^{min} , and P_d^{max} are the minimum and maximum generation limits of DG. $\Lambda_{d,t}^M$ is the LMP of the bus on which the DG is present. The value of $\Lambda_{d,t}^S$ is decided by the DSO to maintain the network parameters within limits. The $\Lambda_{d,t}^S$ may be equal to or greater than the $\Lambda_{d,t}^M$. The bidding price, $\Lambda_{d,t}^{MBid}$, offered by DGs to DSO in the main market and the bidding price, $\Lambda_{d,t}^{SBid}$, for the supplementary operations are given by,

$$\Lambda_{d,t}^{MBid} = \max\{(c_d^b + 2c_d^c P_{d,t}^M), \Lambda_{d,t}^M\}, \quad \text{and} \quad (6.29)$$

$$\Lambda_{d,t}^{SBid} = \max\{(c_d^b + 2c_d^c(P_{d,t}^M + P_{d,t}^S)), \Lambda_{d,t}^S\}. \quad (6.30)$$

For the main market, variables are optimised by keeping the supplementary operations variables at zero. In the case of supplementary operations, the variables are optimised by keeping the variables of the main market at their previous values.

6.2.5 DSO

The DSO maintains the network constraints and clears the local energy market considering the load demand at different buses, net power injection by VCs, and bids offered by DGs. DSO determines the LMPs of various buses based on the optimum power flow. It clears the DGs bids in the main market and supplementary operations using factors $\Omega_{d,t}^M$ and $\Omega_{d,t}^S$, respectively, such that $0 \leq \Omega_{d,t}^M, \Omega_{d,t}^S \leq 1$. Thus, the cost function of the DSO, C^{DSO} , can be written as,

$$C^{DSO} = \sum_{t=1}^T [\Lambda_t^{G,P} P_{1,t}^G + \Lambda_t^{G,Q} |Q_{1,t}^G| + \sum_{d=1}^{N_d} (\Omega_{d,t}^M \Lambda_{d,t}^{MBid} P_{d,t}^M + \Omega_{d,t}^S \Lambda_{d,t}^{SBid} P_{d,t}^S)]. \quad (6.31)$$

The $|Q_{1,t}^G|$ can make the problem non-convex. So, instead of $|Q_{1,t}^G|$, in this framework $Q_{1,t}^{Gaux}$ is used in this framework such that $Q_{1,t}^{Gaux} \geq -Q_{1,t}^G$, $Q_{1,t}^{Gaux} \geq Q_{1,t}^G$ and $Q_{1,t}^{Gaux} \geq 0$. The DSO level optimisation is constrained by the following equations.

$$\sum_{k=1}^{N^B} P_{k,t}^G - \sum_{k=1}^{N^B} P_{k,t}^D = 0 \quad : \lambda_t^1 \quad (6.32)$$

$$\sum_{k=1}^{N^B} Q_{k,t}^G - \sum_{k=1}^{N^B} Q_{k,t}^D = - \sum_{k'=1}^{N^B} b_{k'k} \quad : \lambda_t^2 \quad (6.33)$$

The constraints for active and reactive power balance at each time interval are given by (6.32) and (6.33). The binary parameters $x_{k,n}^C$, $x_{k,d}^{DG}$, and x_k^{PCC} indicate the presence of VC, DG, and point of common coupling (PCC), respectively at k^{th} bus. Thus, at bus k , the total active power generation and demand are given by,

$$P_{k,t}^G = x_k^{PCC} P_t^G + \sum_{d=1}^{N^{DG}} x_{k,d}^{DG} (\Omega_{d,t}^M P_{d,t}^M + \Omega_{d,t}^S P_{d,t}^S), \quad \text{and} \quad (6.34)$$

$$P_{k,t}^D = P_{k,t}^{FD} + \sum_{n=1}^{N^c} x_{k,n}^C P_{n,t}^{net}. \quad (6.35)$$

The net injection of n^{th} VC is given by $P_{n,t}^{net}$ that consists of the power exchange of n^{th} VC with the utility and other VCs. Similarly, the total reactive power generation and demand can be expressed for all the buses. Other Constraints related to DSO can be expressed as follows.

$$-P_l^{max} \leq \sum_{k=1}^{N^B} f_{l-k}^{P-P} (P_{k,t}^G - P_{k,t}^D) + \sum_{k=1}^{N^B} f_{l-k}^{P-Q} (Q_{k,t}^G - Q_{k,t}^D) \leq P_l^{max} \quad : \mu_{l,t}^1, \mu_{l,t}^2 \quad \forall l \quad (6.36)$$

$$V^{min} \leq \sum_{k=1}^{N^B} X_{N^B+k',k} (P_{k,t}^G - P_{k,t}^D) + \sum_{k=1}^{N^B} X_{N^B+k',N^B+k} (Q_{k,t}^G - Q_{k,t}^D) \leq V^{max} : \mu_{k',t}^3, \mu_{k',t}^4 \quad \forall k' \quad (6.37)$$

$$P_{min}^G \leq P_t^G \leq P_{max}^G : \mu_t^5, \mu_t^6 \quad (6.38)$$

$$Q_{min}^G \leq Q_t^G \leq Q_{max}^G : \mu_t^7, \mu_t^8 \quad (6.39)$$

The constraint (6.36) gives the line limits in terms of generation shift distribution (GSD) factors. The GSD factors, f_{l-k}^{P-P} and f_{l-k}^{P-Q} , have been discussed in Appendix I and are taken from [81]. At each bus, the limits for voltage magnitude are given by (6.37). As described in Appendix I, the term $X_{k,k'}$ is based on the network topology. The equations (6.38) and (6.39) limit the active and reactive power exchanges, respectively, at PCC. For the DSO, the Lagrangian function is given by the equation ¹. In the proposed formulation to evaluate the savings of participants, the reactive power exchange of VCs with the distribution network has not been considered. Hence, only LMP based on active power can be considered in this problem formulation. The partial derivative of the Lagrangian function in respect of power demand at bus k is used as active power LMP at k^{th} bus and is given by

$$\lambda_{t,k}^{LMP} = \lambda_t^1 + \sum_l (-\mu_{l,t}^1 + \mu_{l,t}^2) f_{l-k}^{P-P} + \sum_{k'} (-\mu_{k',t}^3 + \mu_{k',t}^4) X_{N^B+k',k}. \quad (6.40)$$

1

$$\begin{aligned} L = \sum_{t=1}^T \left[C^{DSO} - \lambda_t^1 \left(\sum_{k=1}^{N^B} P_{k,t}^G - \sum_{k=1}^{N^B} P_{k,t}^D \right) - \lambda_t^2 \left(\sum_{k=1}^{N^B} Q_{k,t}^G - \sum_{k=1}^{N^B} Q_{k,t}^D + \sum_{k'=1}^{N^B} b_{k'k'} \right) \right. \\ - \sum_l \mu_{l,t}^1 \left(-P_l^{max} - \sum_{k=1}^{N^B} f_{l-k}^{P-P} (P_{k,t}^G - P_{k,t}^D) - \sum_{k=1}^{N^B} f_{l-k}^{P-Q} (Q_{k,t}^G - Q_{k,t}^D) \right) \\ - \sum_l \mu_{l,t}^2 \left(-P_l^{max} + \sum_{k=1}^{N^B} f_{l-k}^{P-P} (P_{k,t}^G - P_{k,t}^D) + \sum_{k=1}^{N^B} f_{l-k}^{P-Q} (Q_{k,t}^G - Q_{k,t}^D) \right) \\ - \sum_{k'} \mu_{k',t}^3 \left(V^{min} - \sum_{k=1}^{N^B} X_{N^B+k',k} (P_{k,t}^G - P_{k,t}^D) - \sum_{k=1}^{N^B} X_{N^B+k',N^B+k} (Q_{k,t}^G - Q_{k,t}^D) \right) \\ - \sum_{k'} \mu_{k',t}^4 \left(-V^{max} + \sum_{k=1}^{N^B} X_{N^B+k',k} (P_{k,t}^G - P_{k,t}^D) + \sum_{k=1}^{N^B} X_{N^B+k',N^B+k} (Q_{k,t}^G - Q_{k,t}^D) \right) \\ \left. - \mu_t^5 (P_{min}^G - P_t^G) - \mu_t^6 (-P_{max}^G + P_t^G) - \mu_t^7 (Q_{min}^G - Q_t^G) - \mu_t^8 (-Q_{max}^G + Q_t^G) \right] \end{aligned}$$

6.3 Methodology

Hong's 2p point estimate method (PEM) [77] accounts for the uncertainties associated with RESs. Section 2.9 describes Hong's 2p PEM to determine the expected scheduled power exchange with other buildings and VCs. In subsequent sections, only the cost function is denoted by $\mathbb{E}(\cdot)$ instead of all variables for simplicity. However, these are the expected values of the variables. ADMM-based decentralised optimisation is used to find the solution to the cooperative game developed in section 6.3.1. The market clearing algorithm, including the operation of DSO, is discussed in section 6.3.2.

6.3.1 The cooperative game formulation

For P2P sharing between buildings and VCs, a cooperative game can be described as given in Table 6.1. The game is played in two levels due to the presence of B2C coupled variables.

Table 6.1: DESCRIPTION OF THE COOPERATIVE GAME

Levels	Players	Strategies	Objectives
1	Buildings	$X_{n,i,t}^b := (P_{n,i,t}^{ls}, P_{n,i,t}^{HVAC}, P_{n,i,j,t}^{b2b}, P_{n,i,t}^{b2c}, \pi_{n,i,j}^{b2b}, \pi_{n,i}^{b2c})$	$C_{n,i}^b$
2	VCs	$X_{n,t}^c := (P_{n,t}^b, P_{n,t}^s, P_{n,t}^{ch}, P_{n,t}^{dis}, P_{n,m,t}^{c2c}, \pi_{n,m}^{c2c})$	C_n^c

It should be noted that VCs act as non-profit-based entities for their buildings, whereas they operate as profit-based entities in C2C trading. Therefore, the VC is a player in C2C trading only. The cooperative game among the buildings of a VC is used for B2B trading and sharing the VC resources. The total cost/benefit of the VC is also to be shared by buildings. To fairly distribute the expected cost savings among players, a modified Nash bargaining problem (MNBP), known as Kalai–Smorodinsky (KS) bargaining solution [83, 84] is formulated and solved in a decentralised manner using an ADMM-based algorithm.

Thus, the required MNBP for P2P trading can be written as

$$\mathcal{F}_1 : \max \left[\prod_{n=1}^{N^c} \left\{ \prod_{i=1}^{N_n^b} (\mathbb{E}(C_{n,i}^{b0}) - \mathbb{E}(C_{n,i}^b)) (\mathbb{E}(C_n^{c0}) - \mathbb{E}(C_n^c)) \right\} \right]. \quad (6.41)$$

subject to:

$$\mathbb{E}(C_{n,i}^{b0}) - \mathbb{E}(C_{n,i}^b) = K_{n,i}^{b2b} (\mathbb{E}(C_{n,i}^{b0}) - \mathbb{E}(C_{n,i}^{b*})), \quad (6.42)$$

$$\mathbb{E}(C_n^{c0}) - \mathbb{E}(C_n^c) = K_n^{c2c} (\mathbb{E}(C_n^{c0}) - \mathbb{E}(C_n^{c*})), \quad (6.43)$$

$$K_{n,i}^{b2b} = K_{n,j}^{b2b}, \quad j = 1, 2, \dots, N_n^b \quad (6.44)$$

$$K_n^{c2c} = K_m^{c2c}, \quad m = 1, 2, \dots, N^c. \quad (6.45)$$

Here, $\mathbb{E}(C_{n,i}^{b*})$ and $\mathbb{E}(C_n^{c*})$ are the best-expected costs in which the price of energy import in P2P trading is equal to the price of energy selling to the utility while the price of energy export to peers is equal to the price of energy buying from the utility. The $K_{n,i}^{b2b}$ and K_n^{c2c} variables are used to ensure that the ratio of cost reduction in the optimal solution to cost reduction in best solution remains the same for all participants in the coalition. Thus, $K_{n,i}^{b2b}$ and K_n^{c2c} will also be considered as one of the strategies for the buildings and the VCs, respectively. In order to maintain the convexity of the problem, $\mathbb{E}(C_{n,i}^{b*})$ and $\mathbb{E}(C_n^{c*})$ are calculated based on the previous iteration values of all the strategies.

”The grand coalition must be in the core for the stability of the coalition [85]”. The core is defined as the set of profit or payoff vectors such that buildings can not improve their payoff by forming another coalition after leaving the grand coalition. The payoff of an individual building can be defined as $\log(1 + \mathbb{E}(C_{n,i}^{b0}) - \mathbb{E}(C_{n,i}^b))$. Let \mathbb{S} be the sub-coalition of this grand coalition. Assume the buildings of \mathbb{S} form a separate coalition such that they receive a better incentive than that they receive on being in a grand coalition as

$$\log(1 + \mathbb{E}(C_{n,i}^{b0}) - \mathbb{E}(C_{n,i}^b)) \leq \log(1 + \mathbb{E}(C_{n,i}^{b0}) - \mathbb{E}(C_{n,i}^{b'})), \quad \forall i \in \mathbb{S} \quad (6.46)$$

Here $C_{n,i}^{b'}$ is the cost function of i^{th} building ($i \in \mathbb{S}$) that has left the grand coalition. In (6.46), to sustain the inequality $C_{n,i}^{b'}$ must be less than $C_{n,i}^b$. This is not possible because the more buildings there are, the more opportunities are available to sell or buy excess renewable energy at a better price than the utility. This means (6.46) is invalid. Thus, the buildings in \mathbb{S} will not leave the grand coalition [85]. The problem \mathcal{F}_1 can be redefined as a minimisation problem as follows,

$$\mathcal{F}_2 : \min \left[- \sum_{n=1}^{N^c} \left\{ \sum_{i=1}^{N_n^b} \log(1 + \mathbb{E}(C_{n,i}^{b0}) - \mathbb{E}(C_{n,i}^b)) + \log(1 + \mathbb{E}(C_n^{c0}) - \mathbb{E}(C_n^c)) \right\} \right]. \quad (6.47)$$

Algorithm 5: Algorithm for P2P Energy Scheduling and Incentive distribution

- 1 Initialize $\tau = 1$, $\sigma(1)$, and $\omega(1) = 0$
- 2 Set δ, τ, ν
- 3 Repeat

4 For each VC

—Building-level optimisation—

5 For each building

6 $Solve_{X^b \in \gamma_b} \mathcal{F}_3(X^b, \sigma^{b2b}(\tau), \omega^{b2b}(\tau), \sigma^{b2c}(\tau), \omega^{b2c}(\tau))$

7 End for.

8 Update σ^{b2b} :

9 $Solve_{\sigma^{b2b} \in \gamma_b} \mathcal{F}_3(X^b(\tau + 1), \sigma^{b2b}, \omega^{b2b}(\tau))$

10 $\omega^{b2b}(\tau + 1) = \omega^{b2b}(\tau) + \delta^{b2b}(\tau)(X^{b2b}(\tau + 1) - \sigma^{b2b}(\tau + 1))$

—VC-level optimisation—

11 $Solve_{(X^c, \sigma^{c2c}) \in \gamma_c} \mathcal{F}_3(X^c, \sigma^{c2c}(\tau), \omega^{c2c}(\tau), \sigma^{b2c}, \omega^{b2c}(\tau))$

12 $\omega^{b2c}(\tau + 1) = \omega^{b2c}(\tau) + \delta^{b2c}(\tau)(X^{b2c}(\tau + 1) - \sigma^{b2c}(\tau + 1))$

13 End for.

14 Update σ^{c2c} :

15 $Solve_{\sigma^{c2c} \in \gamma_2} \mathcal{F}_3(X^c(\tau + 1), \sigma^{c2c}, \omega^{c2c}(\tau))$

16 $\omega^{c2c}(\tau + 1) = \omega^{c2c}(\tau) + \delta^{c2c}(\tau)(X^{c2c}(\tau + 1) - \sigma^{c2c}(\tau + 1))$

—Penalty-parameter update—

17 Calculate λ^P and λ^D :

18 $\lambda^P = \|X(\tau + 1) - \sigma(\tau + 1)\|$

19 $\lambda^D = \|\sigma(\tau + 1) - \sigma(\tau)\|$

20 Update δ by,

21
$$\delta(\tau + 1) = \begin{cases} \delta(\tau)/\nu, & \text{if } \lambda^P < \tau\lambda^D, \\ \nu\delta(\tau), & \text{if } \lambda^P > \frac{\lambda^D}{\tau}, \\ \delta(\tau), & \text{otherwise.} \end{cases}$$

22 $\tau = \tau + 1$

23 Until $\|\omega_1(\tau) - \omega_1(\tau - 1)\| < tolerance$

The problem \mathcal{F}_2 has some coupling constraints as (6.10), (6.11), (6.23), (6.24), (6.25), (6.26), (6.44), and (6.45). These coupling constraints must be decoupled to solve \mathcal{F}_2 in a decentralised manner. ADMM [76] can be used for decentralisation by introducing the auxiliary variables $(\sigma_{n,i,j,t}^{P_{b2b}}, \sigma_{n,i,j,t}^{\pi_{b2b}}, \sigma_{n,m,t}^{P_{c2c}}, \sigma_{n,m,t}^{\pi_{c2c}}, \sigma_{n,i,t}^{P_{b2c}}, \sigma_{n,i,t}^{\pi_{b2c}}, \sigma_{n,i}^{K^{b2b}}, \text{ and } \sigma_n^{K^{c2c}})$ corresponding to main variables $(P_{n,i,j,t}^{b2b}, \pi_{n,i,j,t}^{b2b}, P_{n,m,t}^{c2c}, \pi_{n,m,t}^{c2c}, P_{n,i,t}^{b2c}, \pi_{n,i,t}^{b2c}, K_{n,i}^{b2b}, \text{ and } K_n^{c2c})$. Now the coupling

constraints can be re-written as,

$$\sigma_{n,i,j,t}^{P_{b2b}} + \sigma_{n,j,i,t}^{P_{b2b}} = 0, \quad (6.48)$$

$$\sigma_{n,i,j}^{\pi_{b2b}} + \sigma_{n,j,i}^{\pi_{b2b}} = 0, \quad (6.49)$$

$$\sigma_{n,m,t}^{P_{c2c}} + \sigma_{m,n,t}^{P_{c2c}} = 0, \quad (6.50)$$

$$\sigma_{n,m}^{\pi_{c2c}} + \sigma_{m,n}^{\pi_{c2c}} = 0, \quad (6.51)$$

$$\sigma_{n,i}^{K^{b2b}} = \sigma_{n,j}^{K^{b2b}}, \quad j = 1, 2, \dots, N_n^b \quad (6.52)$$

$$\sigma_n^{K^{c2c}} = \sigma_m^{K^{c2c}}, \quad m = 1, 2, \dots, N^c \quad (6.53)$$

$$P_{n,t}^b - P_{n,t}^s + P_{n,t}^{dis} - P_{n,t}^{ch} + \sum_{\substack{m=1 \\ m \neq n}}^{N^c} P_{n,m,t}^{c2c} = \sum_{i=1}^{N_n^b} \sigma_{n,i,t}^{P_{b2c}}, \quad \text{and} \quad (6.54)$$

$$C_n^c = \sum_{i=1}^{N_n^b} \sigma_{n,i}^{\pi_{b2c}}. \quad (6.55)$$

The function \mathcal{F}_2 in eq. (6.47) can be re-defined as follows based on the reformulation of coupling constraints.

$$\begin{aligned} \mathcal{F}_3 : \min & \left\{ - \left[\sum_{n=1}^{N^c} \left\{ \sum_{i=1}^{N_n^b} \log(1 + \mathbb{E}(C_{n,i}^{b0}) - \mathbb{E}(C_{n,i}^b)) + \log(1 + \mathbb{E}(C_n^{c0}) - \mathbb{E}(C_n^c)) \right\} \right] + \right. \\ & \sum_{n=1}^{N^c} \sum_{i=1}^{N_n^b} \sum_{\substack{j=1 \\ j \neq i}}^{N_n^b} \left[\sum_{t=1}^T \frac{\delta_1}{2} \left(P_{n,i,j,t}^{b2b} - \sigma_{n,i,j,t}^{P_{b2b}} + \frac{\omega_{n,i,j,t}^{P_{b2b}}}{\delta_1} \right)^2 + \frac{\delta_2}{2} \left(\pi_{n,i,j}^{b2b} - \sigma_{n,i,j}^{\pi_{b2b}} + \frac{\omega_{n,i,j}^{\pi_{b2b}}}{\delta_2} \right)^2 \right] + \\ & \sum_{n=1}^{N^c} \sum_{i=1}^{N_n^b} \frac{\delta_{12}}{2} \left(K_{n,i}^{b2b} - \sigma_{n,i}^{K^{b2b}} + \frac{\omega_{n,i}^{K^{b2b}}}{\delta_{12}} \right)^2 + \sum_{n=1}^{N^c} \sum_{i=1}^{N_n^b} \left[\sum_{t=1}^T \frac{\delta_3}{2} \left(P_{n,i,t}^{b2c} - \sigma_{n,i,t}^{P_{b2c}} + \frac{\omega_{n,i,t}^{P_{b2c}}}{\delta_3} \right)^2 + \right. \\ & \left. \frac{\delta_4}{2} \left(\pi_{n,i}^{b2c} - \sigma_{n,i}^{\pi_{b2c}} + \frac{\omega_{n,i}^{\pi_{b2c}}}{\delta_4} \right)^2 \right] + \sum_{n=1}^{N^c} \left[\sum_{\substack{m=1 \\ m \neq n}}^{N^c} \left\{ \sum_{t=1}^T \frac{\delta_5}{2} \left(P_{n,m,t}^{c2c} - \sigma_{n,m,t}^{P_{c2c}} + \frac{\omega_{n,m,t}^{P_{c2c}}}{\delta_5} \right)^2 \right. \right. \\ & \left. \left. + \frac{\delta_6}{2} \left(\pi_{n,m}^{c2c} - \sigma_{n,m}^{\pi_{c2c}} + \frac{\omega_{n,m}^{\pi_{c2c}}}{\delta_6} \right)^2 \right\} + \frac{\delta_{56}}{2} \left(K_n^{c2c} - \sigma_n^{K^{c2c}} + \frac{\omega_n^{K^{c2c}}}{\delta_{56}} \right)^2 \right] \left. \right\}. \quad (6.56) \end{aligned}$$

The minimisation problem \mathcal{F}_3 is subjected to constraints γ_b , γ_c , γ_1 , and γ_2 . Here, $\gamma_b := [(6.6), (6.7), (6.8), (6.9), (6.12), (6.13)]$, $\gamma_c := [P^b \geq 0, P^s \geq 0, (6.18), (6.19), (6.20), (6.21), (6.22), (6.54), (6.55)]$, $\gamma_1 := [(6.48), (6.49), (6.52)]$, and $\gamma_2 := [(6.50), (6.51), (6.53)]$. The problem \mathcal{F}_3 can be solved by using the steps given in Algorithm 5. After the initialization, in step 6

of Algorithm 5, for i^{th} building of n^{th} VC, (6.56) can be re-written as:

$$\begin{aligned} \mathcal{F}_4 : \min & \left\{ -\log(1 + \mathbb{E}(C_{n,i}^{b0}) - \mathbb{E}(C_{n,i}^b)) + \sum_{\substack{j=1 \\ j \neq i}}^{N_n^b} \left[\sum_{t=1}^T \frac{\delta_1}{2} \left(P_{n,i,j,t}^{b2b} - \sigma_{n,i,j,t}^{P_{b2b}} + \frac{\omega_{n,i,j,t}^{P_{b2b}}}{\delta_1} \right)^2 + \right. \right. \\ & \left. \frac{\delta_2}{2} \left(\pi_{n,i,j}^{b2b} - \sigma_{n,i,j}^{\pi_{b2b}} + \frac{\omega_{n,i,j}^{\pi_{b2b}}}{\delta_2} \right)^2 \right] + \frac{\delta_{12}}{2} \left(K_{n,i}^{b2b} - \sigma_{n,i}^{K^{b2b}} + \frac{\omega_{n,i}^{K^{b2b}}}{\delta_{12}} \right)^2 + \\ & \left. \sum_{t=1}^T \frac{\delta_3}{2} \left(P_{n,i,t}^{b2c} - \sigma_{n,i,t}^{P_{b2c}} + \frac{\omega_{n,i,t}^{P_{b2c}}}{\delta_3} \right)^2 + \frac{\delta_4}{2} \left(\pi_{n,i}^{b2c} - \sigma_{n,i}^{\pi_{b2c}} + \frac{\omega_{n,i}^{\pi_{b2c}}}{\delta_4} \right)^2 \right\}. \end{aligned} \quad (6.57)$$

For B2B auxiliary variable update in step 9 of Algorithm 5 for n^{th} VC, (6.56) can be re-written as:

$$\begin{aligned} \mathcal{F}_5 : \min & \left\{ \sum_{i=1}^{N_n^b} \sum_{\substack{j=1 \\ j \neq i}}^{N_n^b} \left[\sum_{t=1}^T \frac{\delta_1}{2} \left(P_{n,i,j,t}^{b2b} - \sigma_{n,i,j,t}^{P_{b2b}} + \frac{\omega_{n,i,j,t}^{P_{b2b}}}{\delta_1} \right)^2 + \frac{\delta_2}{2} \left(\pi_{n,i,j}^{b2b} - \sigma_{n,i,j}^{\pi_{b2b}} + \frac{\omega_{n,i,j}^{\pi_{b2b}}}{\delta_2} \right)^2 \right] + \right. \\ & \left. \sum_{i=1}^{N_n^b} \frac{\delta_{12}}{2} \left(K_{n,i}^{b2b} - \sigma_{n,i}^{K^{b2b}} + \frac{\omega_{n,i}^{K^{b2b}}}{\delta_{12}} \right)^2 + \sum_{i=1}^{N_n^b} \left[\sum_{t=1}^T \frac{\delta_3}{2} \left(P_{n,i,t}^{b2c} - \sigma_{n,i,t}^{P_{b2c}} + \frac{\omega_{n,i,t}^{P_{b2c}}}{\delta_3} \right)^2 \right. \right. \\ & \left. \left. + \frac{\delta_4}{2} \left(\pi_{n,i}^{b2c} - \sigma_{n,i}^{\pi_{b2c}} + \frac{\omega_{n,i}^{\pi_{b2c}}}{\delta_4} \right)^2 \right] \right\}. \end{aligned} \quad (6.58)$$

For VC-level optimisation in step 11 of Algorithm 5 for n^{th} VC, (6.56) can be re-written as:

$$\begin{aligned} \mathcal{F}_6 : \min & \left\{ -\log(1 + \mathbb{E}(C_n^{c0}) - \mathbb{E}(C_n^c)) + \sum_{i=1}^{N_n^b} \left[\sum_{t=1}^T \frac{\delta_3}{2} \left(P_{n,i,t}^{b2c} - \sigma_{n,i,t}^{P_{b2c}} + \frac{\omega_{n,i,t}^{P_{b2c}}}{\delta_3} \right)^2 \right. \right. \\ & \left. + \frac{\delta_4}{2} \left(\pi_{n,i}^{b2c} - \sigma_{n,i}^{\pi_{b2c}} + \frac{\omega_{n,i}^{\pi_{b2c}}}{\delta_4} \right)^2 \right] + \left[\sum_{\substack{m=1 \\ m \neq n}}^{N_c} \left\{ \sum_{t=1}^T \frac{\delta_5}{2} \left(P_{n,m,t}^{c2c} - \sigma_{n,m,t}^{P_{c2c}} + \frac{\omega_{n,m,t}^{P_{c2c}}}{\delta_5} \right)^2 \right. \right. \\ & \left. \left. + \frac{\delta_6}{2} \left(\pi_{n,m}^{c2c} - \sigma_{n,m}^{\pi_{c2c}} + \frac{\omega_{n,m}^{\pi_{c2c}}}{\delta_6} \right)^2 \right\} + \frac{\delta_{56}}{2} \left(K_n^{c2c} - \sigma_n^{K^{c2c}} + \frac{\omega_n^{K^{c2c}}}{\delta_{56}} \right)^2 \right] \right\}. \end{aligned} \quad (6.59)$$

Then, in step 15 of Algorithm 5 for the C2C auxiliary variable update, (6.56) can be re-written as:

$$\begin{aligned} \mathcal{F}_7 : \min & \left\{ \sum_{n=1}^{N_c} \left[\sum_{\substack{m=1 \\ m \neq n}}^{N_c} \left\{ \sum_{t=1}^T \frac{\delta_5}{2} \left(P_{n,m,t}^{c2c} - \sigma_{n,m,t}^{P_{c2c}} + \frac{\omega_{n,m,t}^{P_{c2c}}}{\delta_5} \right)^2 \right. \right. \right. \\ & \left. \left. \frac{\delta_6}{2} \left(\pi_{n,m}^{c2c} - \sigma_{n,m}^{\pi_{c2c}} + \frac{\omega_{n,m}^{\pi_{c2c}}}{\delta_6} \right)^2 \right\} + \frac{\delta_{56}}{2} \left(K_n^{c2c} - \sigma_n^{K^{c2c}} + \frac{\omega_n^{K^{c2c}}}{\delta_{56}} \right)^2 \right] \right\}. \end{aligned} \quad (6.60)$$

After calculating all the power profiles, the VC cloud will send the net-injected power data to the DSO.

6.3.2 Market Operation

The proposed algorithm of market operations is executed sequentially and solved iteratively as depicted in the flowchart shown in Figure 6.2. A separate blockdiagram for understanding the market operation is given in Figure 6.3. Initially, cloud-based computing in VCs decides the net power injection into the distribution network using decentralised P2P trading, as discussed in Algorithm 5. In parallel to this VC-level optimisation, DGs optimise their objectives (6.2.4) for main market bidding by keeping the supplementary operations variables at zero. For clearing the main market, the DSO optimises its problem (6.2.5) by considering the net power injection by the VCs and the bid price and power offered by the DGs. If all network constraints are satisfied, the DSO calculates the LMPs based on the dual variables and GSD factors as discussed in Section 6.2.5. Otherwise, the DSO performs a supplementary operation to satisfy network constraints. In the supplementary operation loop, the DSO increases the LMPs to the DGs with a fixed step size, and the DGs update their supplementary bidding strategies as discussed in (6.2.4). This supplementary operation loop repeats until the network constraints are satisfied. This process ends with the satisfaction of the network constraints and the calculation of the corresponding LMPs. Since the cost of resources to make all transactions feasible is captured by the LMPs, all other variables obtained in the supplementary operation are reset to zero. These newly generated LMPs are used for further processing and communicated to all the VCs and DGs for rescheduling. This process is repeated until the difference in LMPs between the subsequent iterations is within tolerance.

6.4 Simulation Results

An IEEE 33 bus system is considered in this work as given in Appendix II. The data for the VCs/buildings and DGs are given in Table 6.3 and Table 6.4, respectively. Here, $C1$, $C2$, and $C3$ represent the VCs. Each VC has buildings with different load profiles, as shown in Figure 6.4(a). The solar power generation (SPG) for 125kW rated capacity, and wind power generation (WPG) for 100kW rated capacity are given in Figure 6.4(b). The minimum and maximum SOC level for all the shared BESS is considered as 20% and 90%, respectively. Both charging and discharging powers are limited to 50kW/h. The fraction of load supplied (ϵ^{LS}) is assumed as 1 since load curtailment is not considered in this work. Only load shifting is considered up to $\pm 10\%$. The

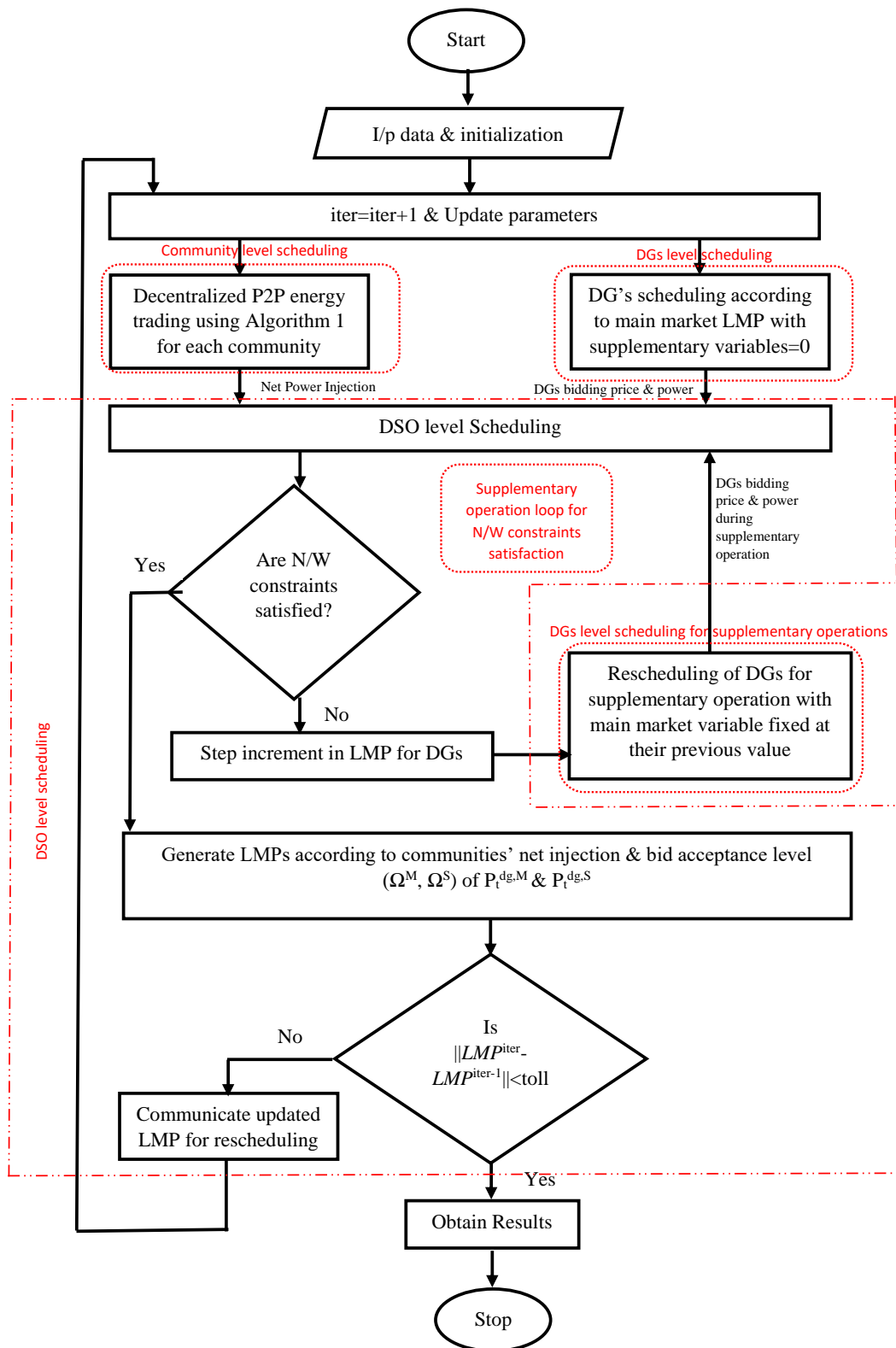


Figure 6.2: FLOWCHART FOR P2P ENERGY SHARING WITH DSO MAINTAINING THE NETWORK PARAMETERS AND DGs PARTICIPATING ACTIVELY.

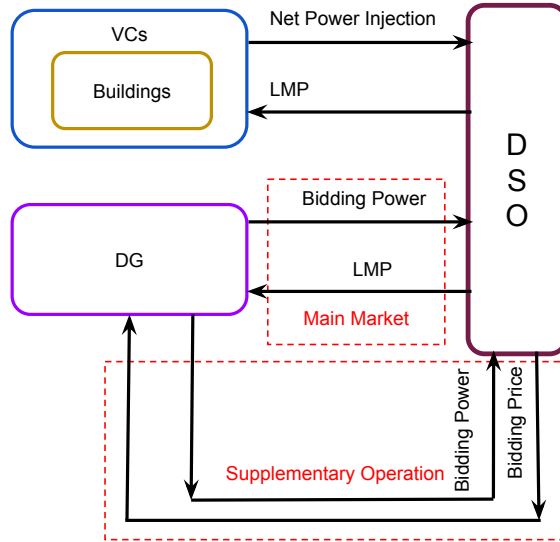


Figure 6.3: BLOCK DIAGRAM FOR MARKET OPERATION

Table 6.3: DATA FOR THE BUILDINGS AND VCs USED IN THIS WORK

	C1			C2			C3		
	B1	B2	B3	B1	B2	B3	B1	B2	B3
Rated Load (kW)	125	125	125	100	125	125	100	100	125
PV rating (kW)	125	125	125	100	125	125	100	100	125
WT rating (kW)	100	100	100	50	100	100	50	50	50
BESS rating (kW)	200			200			200		
Bus Location	21			24			18		

Table 6.4: DATA FOR THE DGs USED IN THIS WORK

	Bus Location	c_d^a (\$)	c_d^b (\$/kW)	c_d^c (\$/kW ²)	P_d^{min} (kW)	P_d^{max} (kW)
DG_1	6	0	0.24	0.0020	0	2000
DG_2	13	0	0.24	0.0025	0	2000

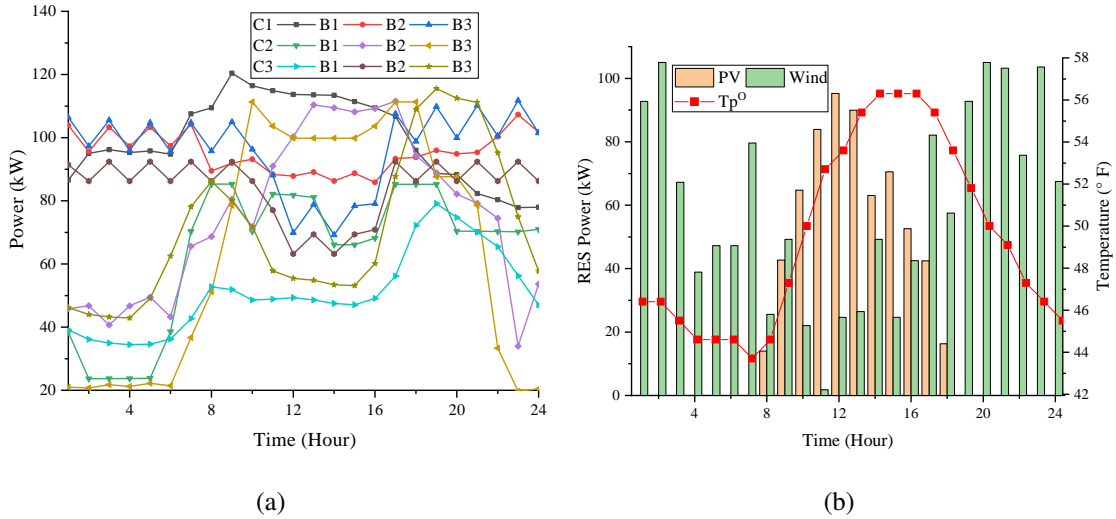


Figure 6.4: (A) LOAD PROFILE OF ALL BUILDINGS (B) ENVIRONMENT'S TEMPERATURE AND RES POWER GENERATION

other parameters are given in Table 6.5. A system with core i3 1.20 GHz processor with 4 GB RAM is used to simulate the work and GAMS/CONOPT4 solver is used for optimisation.

Three different cases have been compared to validate this work:

Case I (Base case): In the base case, the buildings can exchange energy with the utility only to import/export their excess/surplus energy.

Case II: Buildings exchange energy with the VC (B2C) and other buildings (B2B) of that VC in this case. B2C means using shared BESS and importing/exporting from/to the utility.

Case III: This is an extension of the *Case II*. In this case, the VCs can exchange power among themselves through C2C trading. Every C2C energy exchange is accompanied by the addition of an appropriate network utilisation charge.

The base case refers to the absence of almost all the cost-saving features. To analyse the effect of B2B energy sharing and the BESS, *Case II* has been incorporated. The last case, i.e. *Case III*, summarises this work and is used to study the effect of BESS along with that of B2B, B2C, and C2C energy sharing. For all these cases, the different types of costs are compared and summarised in Table 6.6. The total operating costs of buildings, C^b , for *C1*, *C2* and *C3* are 310.67 \$, 130.00 \$, and 522.66 \$, respectively in *Case I*. This is the highest compared to *Case II* and *Case III* because, in this case (*Case I*), buildings can only exchange energy with the utility. To reduce the operating cost in *Case I*, the buildings shift their load according to the available RES generation and the price for power exchange with utility, i.e.,

Table 6.5: VALUES OF PARAMETERS USED

Parameters	Values
η^{ch}	96%
η^{dis}	94.3%
η^{loss}	0.5%
Λ^{UTI}	0.06\$/kW
ϵ^{CE}	0.05\$/kW
Λ^{dis}	0.03\$/kW ²
ϵ_R	4
σ	0.2
τ	0.01
ν	1.5
Λ^{HVAC}	0.003\$/F ²
h^a	0.9602
h^b	0.0398
h^c	0.284 F/kW

Table 6.6: COST (\$) COMPARISON FOR ALL THE THREE CASES OF BUILDINGS

		C1				C2				C3			
		B1	B2	B3	Sum	B1	B2	B3	Sum	B1	B2	B3	Sum
<i>Case I</i>	C^b	109.84	94.21	106.63	310.67	112.37	17.27	0.36	130.00	63.93	282.35	176.38	522.66
<i>Case II</i>	C^{ls}	14.48	14.48	14.48	43.45	16.90	19.96	18.18	55.05	6.80	13.50	9.74	30.05
	C^{HVAC}	8.05	8.05	8.05	24.14	8.36	8.35	8.35	25.06	5.63	5.57	5.53	16.73
	C^{b2b}	3.01	-4.75	1.74	0.00	41.58	-14.42	-27.16	0.00	-61.22	60.02	1.21	0.00
	C^{b2c}	80.56	73.99	78.63	233.18	31.91	-5.49	-14.04	12.38	108.36	188.80	149.94	447.09
	C^b	106.10	91.77	102.91	300.78	98.75	8.41	-14.66	92.49	59.56	267.89	166.42	493.87
<i>Case III</i>	C^{ls}	0.78	0.77	0.78	2.33	1.29	1.29	1.29	3.86	0.67	0.67	0.67	2.01
	C^{HVAC}	2.21	2.14	2.14	6.49	2.36	2.40	2.36	7.12	2.43	2.44	2.47	7.34
	C^{b2b}	1.64	-2.61	0.97	0.00	40.19	-11.08	-29.11	0.00	-59.23	58.35	0.89	0.00
	C^{b2c}	80.70	73.10	77.28	231.08	29.87	-4.32	-16.31	9.25	108.64	187.06	148.74	444.44
	C^b	85.33	73.39	81.17	239.89	73.71	-11.72	-41.77	20.23	52.51	248.52	152.76	453.79

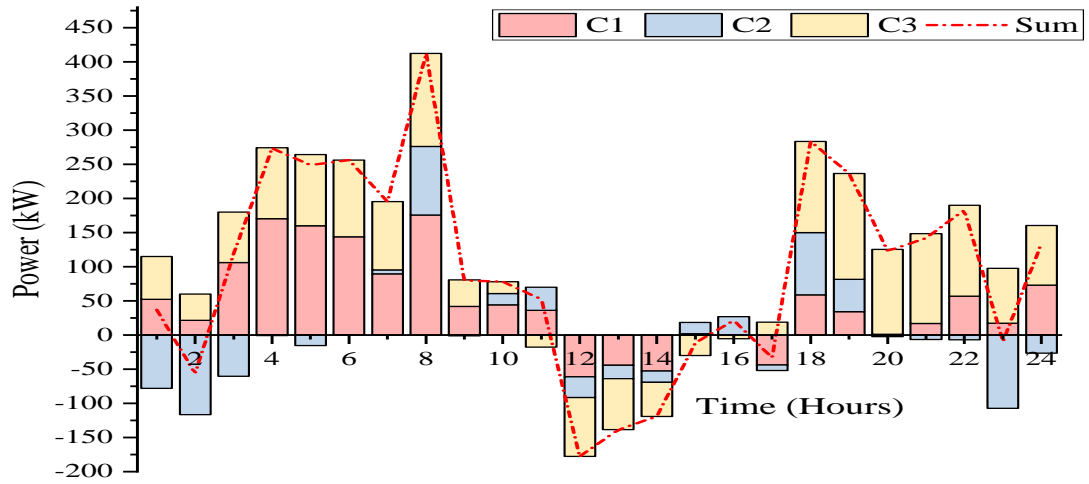
Table 6.7: COST (\$) COMPARISON FOR ALL THE THREE CASES OF VIRTUAL COMMUNITIES

		C1	C2	C3
<i>Case I</i>	C^U	310.67	130.00	522.66
	C^U	218.16	-4.72	430.90
<i>Case II</i>	C^{BESS}	15.02	17.10	16.19
	C^c	233.18	12.38	447.09
<i>Case III</i>	C^U	191.41	45.40	399.65
	C^{BESS}	16.78	14.02	15.79
	C^{e2c}	22.89	-50.17	29.00
	C^c	231.08	9.25	444.44

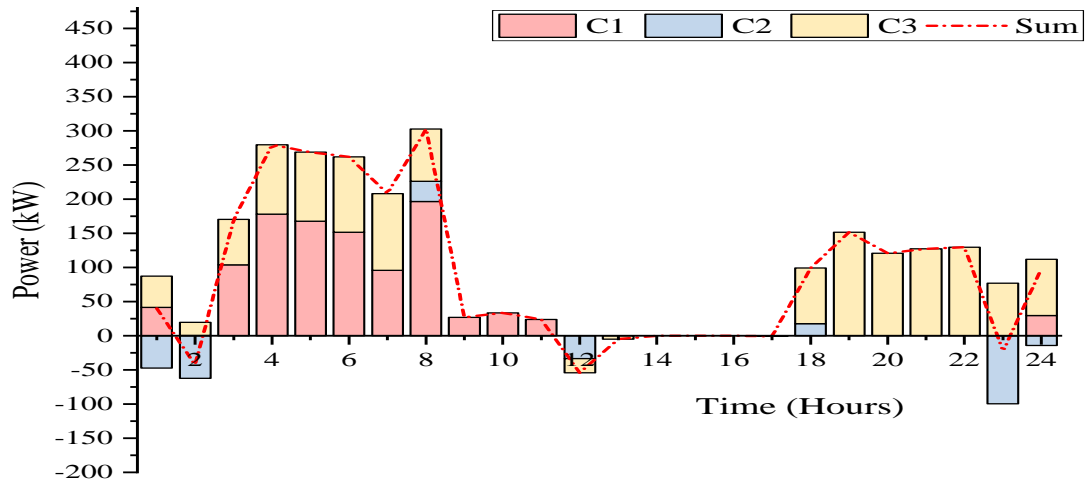
LMP. In *Case II*, buildings can exchange energy with other buildings in B2B trading while simultaneously using the BESS of the VC, taking advantage of load diversity and effective use of RESs. As this consumption of locally available energy increases, the energy exchange with the utility decreases, as shown in Figure 6.5.

As shown in Figure 6.6, the total B2C exchange in *Case II* can be regarded as the algebraic sum of energy exchange with the utility and energy used to charge/discharge the battery. Both the import and export of all VCs have decreased in *Case II* compared to *Case I*. For example, the surplus energy in C2 during 1:00-7:00 hours is exported to the utility in *Case I* (Figure 6.5(a)), while in *Case II* (Figure 6.5(b)) this export decreases because it is used to store in BESS as shown in Figure 6.8. The stored energy is used to supply the load at subsequent intervals, and as a result, imports are also reduced. The cost of B2B trading depends on the building's contribution to P2P transactions as a seller or buyer. For instance, as indicated in the Table 6.6 C^{b2b} is positive for *building 1* of C2, while C^{b2b} is negative for *building 2* and *building 3* of the same VC (C2). This can be analysed from B2B exchange in C2 as depicted in Figure 6.7(b). The *building 1* imports power from other buildings for most of the time intervals, so it pays to the other buildings, and its net cost of B2B trading is positive.

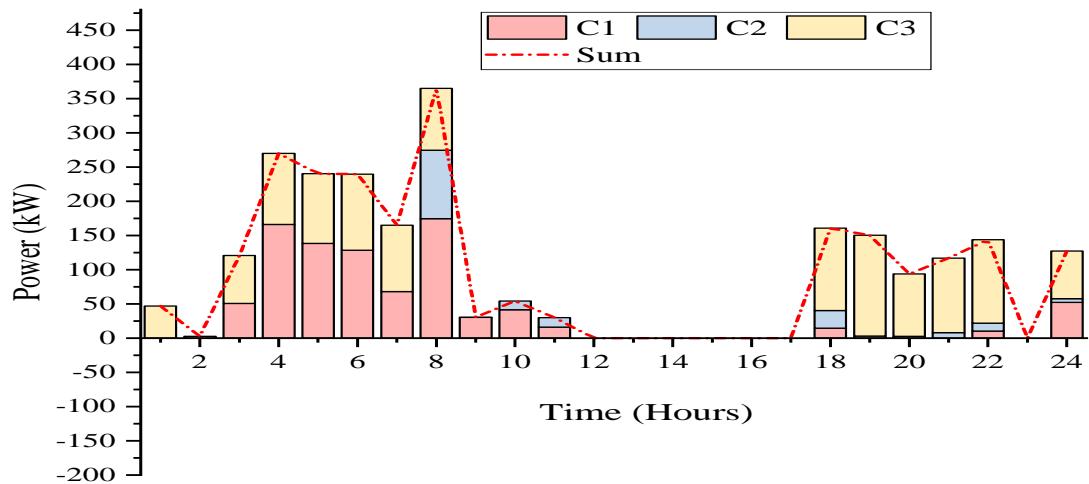
When communities are formed, then along with B2B, B2C energy exchanges also take place. In this case (*Case III*), B2B energy exchanges mostly remain the same as compared to *Case II*. Figure 6.7(b) illustrates that the B2B exchanges in C2 in *Case II* and *Case III* are almost identical. Similarly, B2B exchanges are almost identical in other VCs as well (Figure 6.7). It can also be understood from the cost of B2B exchange, C^{b2b} , in Table 6.6, which is



(a)

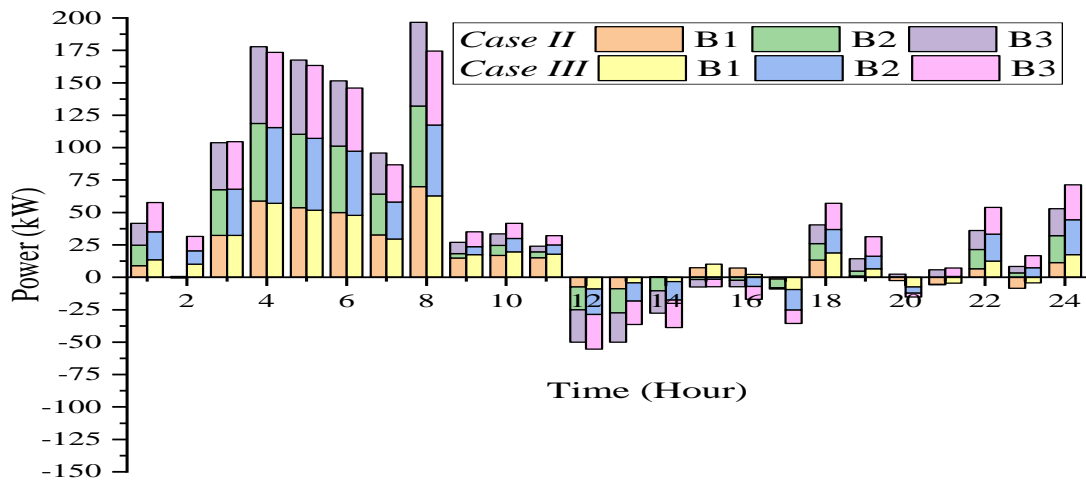


(b)

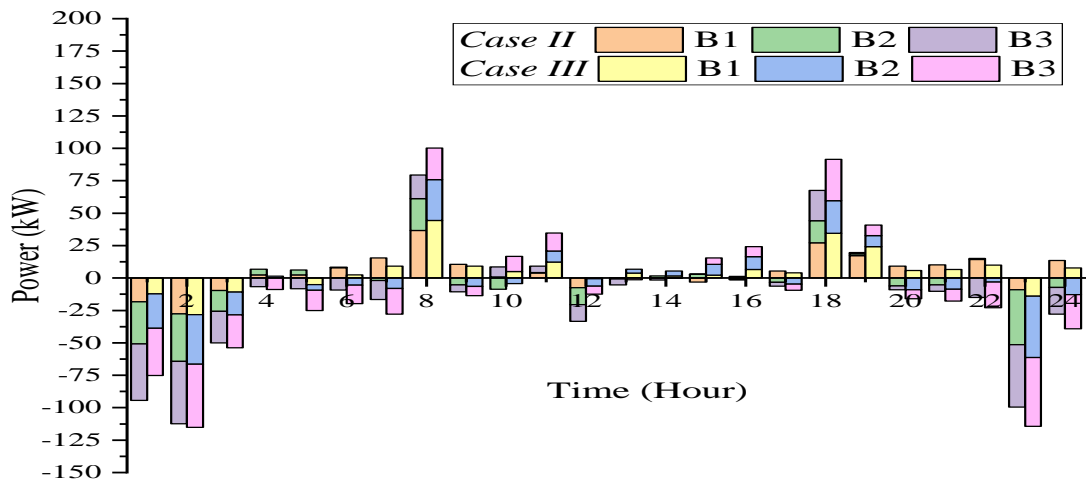


(c)

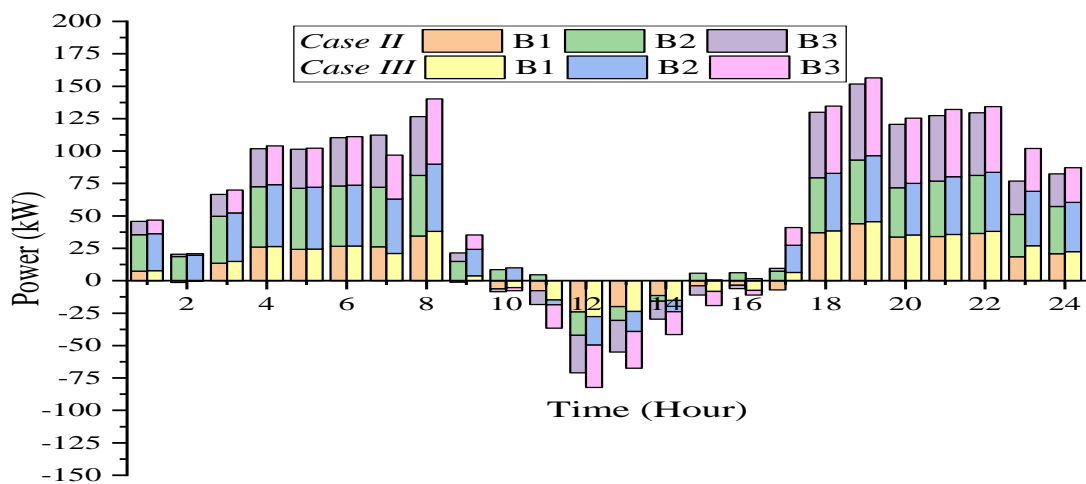
Figure 6.5: POWER EXCHANGE PROFILE OF VCS WITH UTILITY (A) *Case I*, (B) *Case II*, (C) *Case III*



(a)

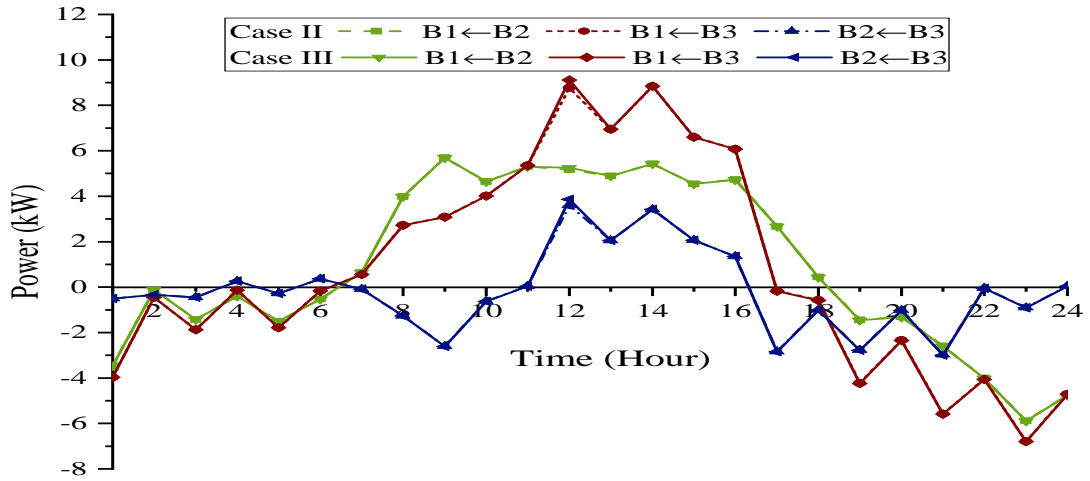


(b)

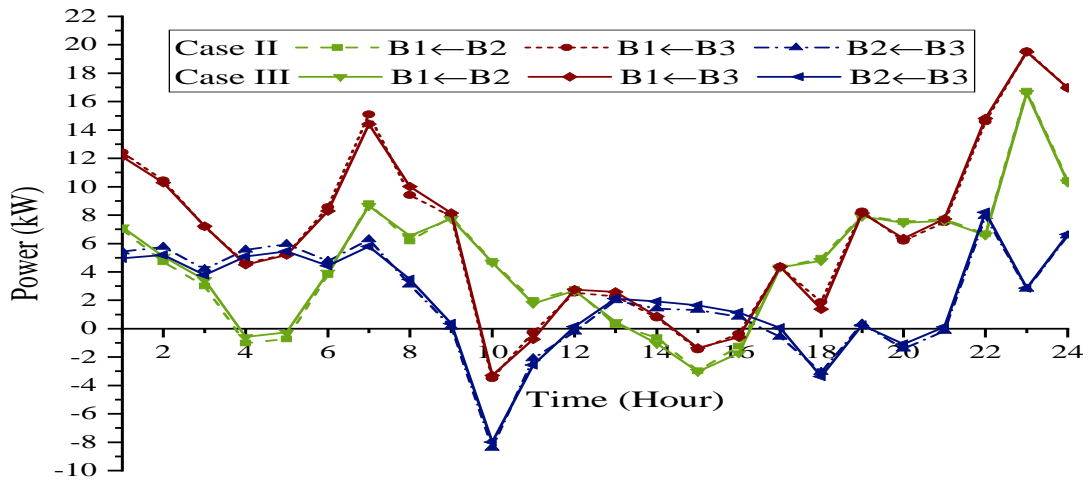


(c)

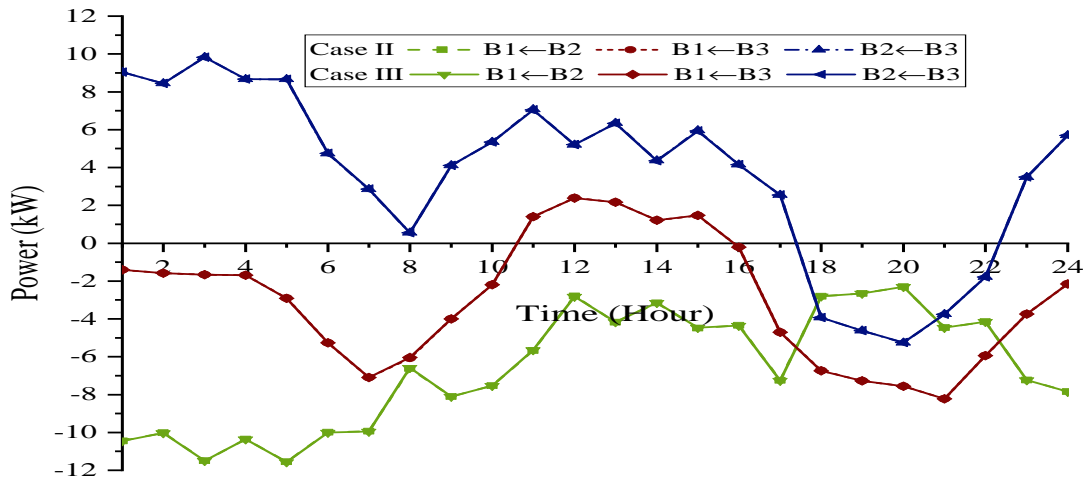
Figure 6.6: B2C POWER EXCHANGE (A) C1, (B) C2, (c) C3



(a)



(b)



(c)

Figure 6.7: B2B Power Exchange for respective virtual communities (A) C1, (B) C2, (C)

C3

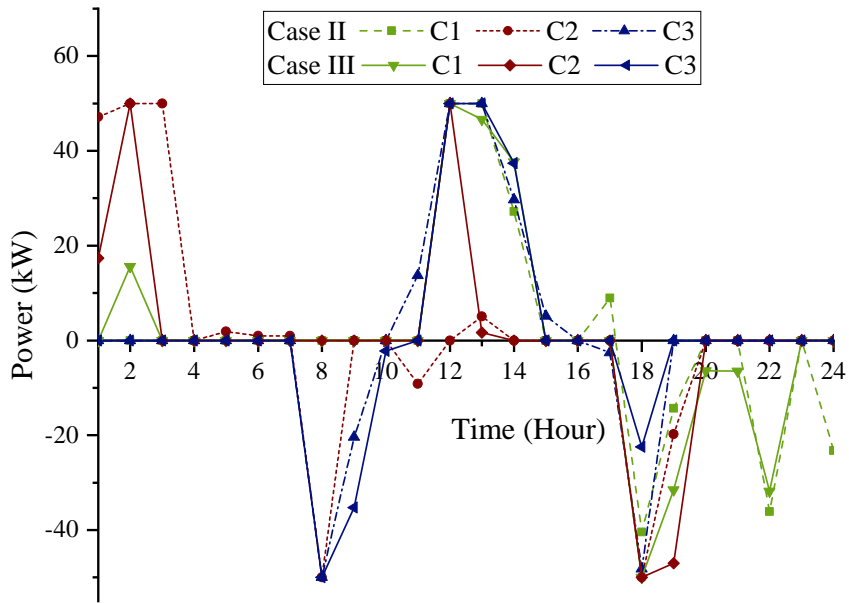


Figure 6.8: BATTERY SCHEDULED POWER

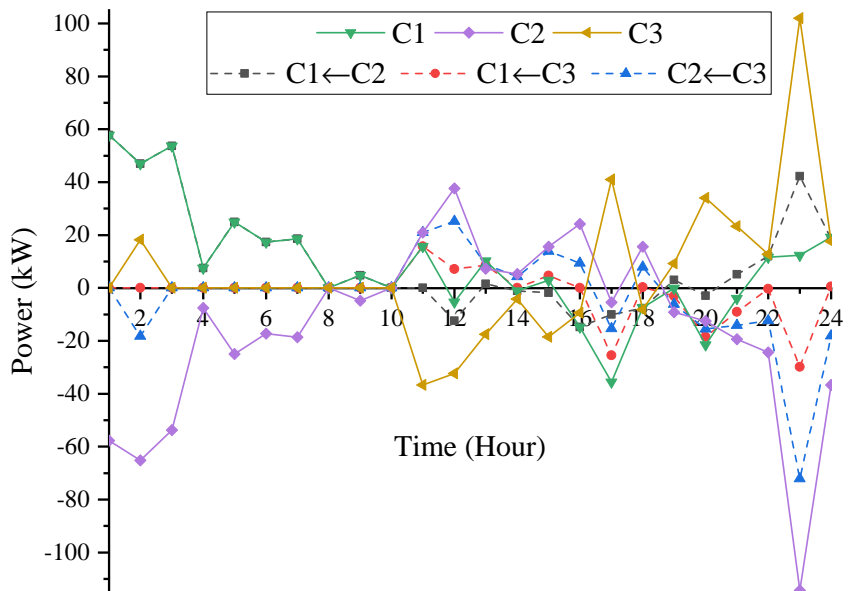


Figure 6.9: C2C NET POWER EXCHANGE (THE SOLID LINE REPRESENTS THE TOTAL POWER IMPORTED/EXPORTED BY THE VC IN C2C ENERGY TRADING, AND THE DASHED LINE IS FOR THEIR RESPECTIVE C2C ENERGY EXCHANGE OF THE VCS.)

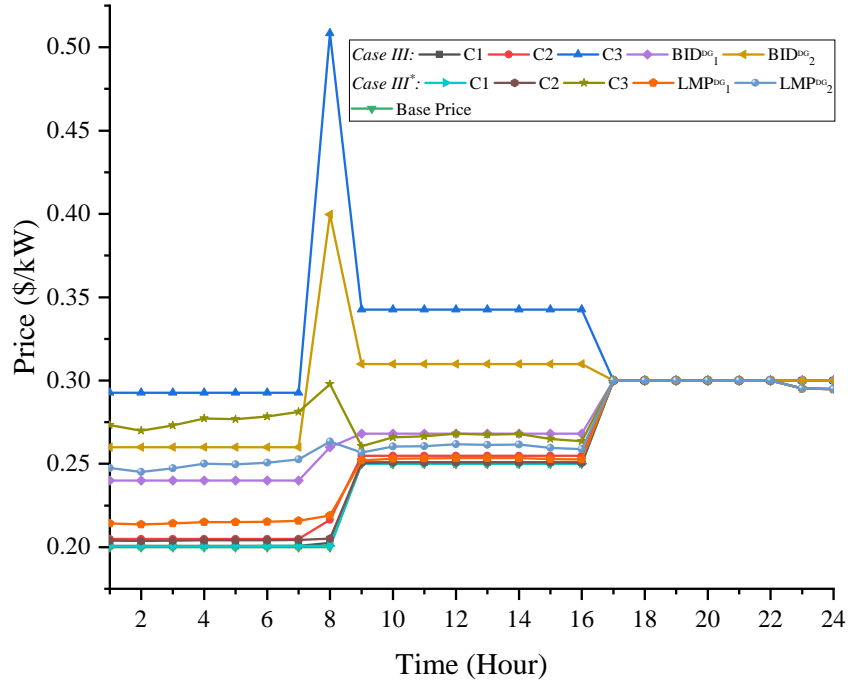
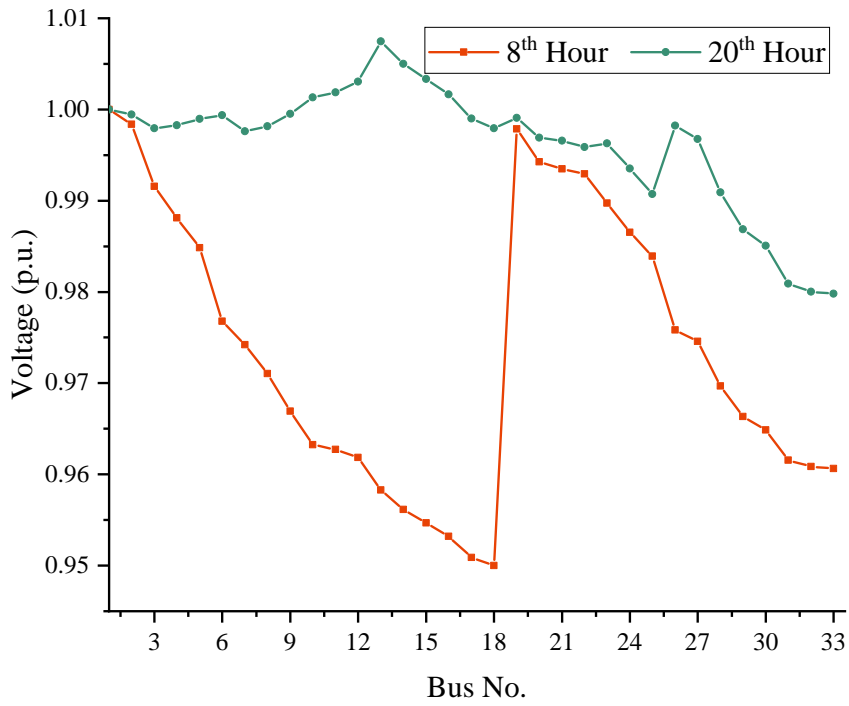
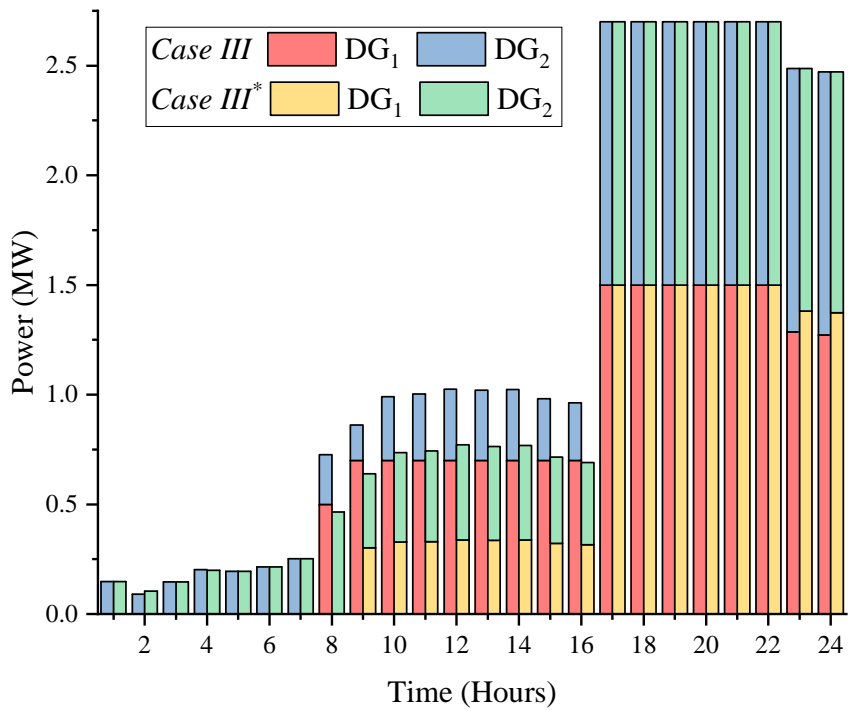


Figure 6.10: LMPs OF THREE VCs, THE BASE PRICE AND THE BIDDING PRICE OF DGs

nearly equal in *Case II* and *Case III*. The C2C trading in *Case III* provides an opportunity for cost savings more effectively by utilising RESs and load diversity. As shown in Figure 6.5(b) and 6.5(c), the total energy export to the utility is almost zero in *Case III* which is much less than 283.43 *kWh* in *Case II*. Similarly, in *Case III* the energy import is 2357.68 *kWh* while in *Case II* it is 2500.29 *kWh*. Also, the cost of user discomfort, C^{ls} , is less in *Case III* than *Case II* as shown in Table 6.6. For *C1*, *C2* and *C3*, decrement in C^{ls} are 94.63%, 92.98%, and 93.31%, respectively in *Case III* compared to *Case II*. Similarly, C^{HVAC} , the discomfort cost due to temperature deviation, is reduced in *Case III* compared to *Case II*. The cause of the reduction in the cost of user discomfort is that the surplus energy of one VC is used by other VCs in *Case III*, rather than being exported to utility or consumed by load shifting as in *Case II*. This load shifting also affects the B2C exchange as shown in Figure 6.6. The energy export by the buildings in *C1* and *C3* increases during 12:00-14:00 hours, which is used by *C2* through C2C transaction (Figure 6.9) to store in BESS (Figure 6.8). This stored energy is used by buildings in *C2* during the 19:00 hour, which shows the increase in energy import in B2C exchange in Figure 6.6(b). The total costs of all the virtual communities for all three cases are given in Table 6.7. For *case III*, the C2C incentives of *C1*, *C2*, and *C3* are 22.83\$, -51.02\$, and 28.20\$ respectively. This C2C incentive, along with the NUC, is the total C^{c2c} cost for *case III* as shown in Table 6.7. The corresponding power exchange is shown in Figure 6.9.



(a)



(b)

Figure 6.11: (A) VOLTAGE PROFILE AT 8th AND 20th HOURS, (B) DGs' CONTRIBUTION

In this work, the power exchange prices are based on LMPs. DSO uses LMPs to maintain the network constraints. For *Case III*, Figure 6.10 shows the LMPs for the VC-buses and the bidding price of DGs. At the 8th hour, there is a spike in the LMP for VC-bus of C3, i.e., bus-18th. This is because the voltage level at this bus during 8th hour is at the minimum operating limit, as shown in Figure 6.11(a). The LMP of C3 is highest as VC-bus 18 is a leaf bus. The voltage level gets improved during late hours, which makes the LMPs and the bidding price almost equal to the base price. For example, the voltage at 20th hour has a comparatively higher margin between the operating and the minimum voltage levels, as shown in Figure 6.11(a). The DSO must use DGs to maintain the voltage within the prescribed range. As the DGs are considered as active participants, they bid according to their marginal cost and LMPs. The DG_2 is placed at bus location 13, which is close to bus location 18; therefore, it can bid higher than DG_1 due to the difference in LMPs. A special case, *Case III**, is also introduced here wherein the DGs are not considered as active participants, i.e., DGs supply power at their marginal price. The profits earned by DG_1 and DG_2 in *Case III* are 4.41 \$ and 4.83 \$, respectively. The powers of DGs are shown in Figure 6.11(b) for both *Case III* and *Case III**. As shown in Figure 6.10, if the active participation of DGs is not considered (*Case III**), LMPs get reduced.

Based on the thesis and the provided search results, the following challenges can be identified in implementing Distributed Generation (DG) participation.

- Technical Integration:
 - Maintaining voltage levels within regulated limits becomes more complex with bidirectional power flow from DGs.
 - Coordinating protection systems and devices to handle reverse power flows.
 - Managing additional cycling and wear on voltage control equipment, especially in rural areas with longer distribution feeders.
- Planning and Operational Challenges:
 - Traditional distribution planning procedures are not adequately designed to account for DG systems.
 - Balancing the goals of increasing DG deployment while minimizing adverse impacts on the distribution system.
 - Incorporating DG into system-wide and distribution-level planning processes.

- Regulatory and Policy Issues:
 - Updating interconnection standards and grid codes to clearly define requirements for DGs.
 - Developing fair and transparent processes for DG interconnection, moving away from 'first-come, first-served' approaches.
- Economic and Market Challenges:
 - Designing appropriate pricing mechanisms and contractual relationships for DG transactions with the grid.
 - Balancing the interests of DG owners, traditional utilities, and non-DG customers.
 - Addressing the potential for cost shifting to non-DG customers.
- Protection and Reliability Concerns:
 - Conventional protection schemes based on overcurrent detection may be insufficient for DG-connected networks.
 - Ensuring selectivity, reliability, and sensitivity of protection schemes in bidirectional power flow scenarios.
 - Developing new protection strategies for active distribution networks and microgrids.
- Communication and Control:
 - Implementing advanced communication systems for coordinating DG operations with the broader grid.
 - Developing control strategies for integrating DG into smart grid operations.
- Market Design and Business Models:
 - Adapting utility business models to accommodate increased DG penetration.
 - Developing new market structures that fairly value DG contributions to the grid.

By addressing these challenges, the integration of DG can be more effectively implemented, leading to a more resilient, efficient, and sustainable power system.

6.5 Summary

A P2P energy transaction framework with the active participation of DGs and prosumers is proposed for a distribution system consisting of several communities. In this chapter, DSO clears the market through the main market and supplementary operations with the active participation of DGs. The cloud-based framework proposed in this work avoids the sharing of any sensitive information between the DSO and the participants and consequently avoids security and privacy issues. The numerical results show that the proposed energy transaction framework is effective. In this LMP-based framework, the cost of energy for all the buildings is reduced significantly (25.9%), and DGs become profitable while maintaining the network constraints. Apart from the financial benefits to the prosumers, the electrical distribution network is also rewarded by peak shaving and reduction in the reverse power flow. The proposed framework considers the uncertainties in RESs usage and takes the advantages of load diversity of all buildings across all the communities. It is observed that the efficacy of this P2P energy transaction framework is enhanced in the presence of shareable BESS.

In this chapter, the BESS helps in dealing with uncertainties arising from renewable generation in day-ahead scheduling. However, in real-time scenarios, it is difficult to incorporate the BESS for the same purpose. In the next chapter, further investigations have been carried out to deal with this issue.